

**Thermal Characterization and Management of Commercially
Available Photovoltaic Cells**

A Final Year Project Report

Presented to

SCHOOL OF MECHANICAL & MANUFACTURING ENGINEERING

Department of Mechanical Engineering

NUST

ISLAMABAD, PAKISTAN

In Partial Fulfillment
of the Requirements for the Degree of
Bachelors of Mechanical Engineering

by

Muhammad Nouman Ihsan

Safwan Nasir

Hassan Jalil

June 10, 2019

EXAMINATION COMMITTEE

We hereby recommend that the final year project report prepared under our supervision by:

NAME Muhammad Nouman Ihsan	REGISTRATION NUMBER. 127283
NAME Safwan Nasir	REGISTRATION NUMBER. 123228
NAME Hassan Jalil	REGISTRATION NUMBER. 128854

Titled: “Thermal Characterization and Management of Commercially Available Photovoltaic Cells” be accepted in partial fulfillment of the requirements for the award of Bachelors of Mechanical Engineering degree with grade ____

Supervisor: Dr. Muhammad Sajid, Assistant Professor SMME, NUST	_____ Dated:
Committee Member: SMME, NUST	_____ Dated:
Committee Member: SMME, NUST	_____ Dated:

(Head of Department)

(Date)

COUNTERSIGNED

Dated: _____
(Dean / Principal)

ABSTRACT

The solar simulator already present in SMME has been redesigned to study the electrical performance of photovoltaic cells with variations in light intensity and temperature, and effect of different thermal management methodologies on efficiency and power output of solar cells. A parabolic reflector has been used with light source along the focal line of parabola to achieve maximum uniformity of light intensity on the targeted plane. Light intensity was measured and it has been found that light intensity can be varied in a range of 800 W/m^2 to 2500 W/m^2 with non-uniformity less than 10%. Hence it lies in the class C of solar simulators. The performance parameters of a solar cell can be determined using a current-voltage curve tracing equipment. The cell temperature at the irradiated surface is measured using an AMG 8833 sensor which is an infrared temperature measuring sensor. The temperature at the dissipative surface of the cell is measured using thermocouples. The effect of temperature variation on the efficiency and maximum power of various kinds of PV cells is studied and to mitigate the depreciative effect of increase in temperature on the electrical performance of cell, different thermal management methodologies such as fins and phase change material are used.

With application of fins and phase change material, significant improvement in the performance of solar cells was recorded. Poly crystalline cells show the maximum efficiency and power output per unit area and at light intensity of 1000 W/m^2 the recorded improvement in efficiency was from 10.02 % to 21.81 % in case of poly-crystalline A type cells using phase change material as a passive cooling methodology.

ACKNOWLEDGMENTS

We would like to express our profound gratitude to our project supervisor Assistant Professor Dr. Muhammad Sajid for, for his patience, encouragement and critique of our work. His continuous theoretical and technical support encouraged and directed this project towards completion.

We are also grateful to the guidance committee members Dr. Jawad Aslam and Lecturer Abdur Rehman for their valuable support in instrumentation and thermal management respectively.

Our heartfelt thanks to Engr. Saeed Iqbal (USP-CASE) for his guidance and assistance in calibration of temperature sensor and design of current and voltage measurement systems.

ORIGINALITY REPORT

We certify that this research work titled “*Thermal characterization and management of commercially available photovoltaic cells*” is our own work. The work has not been presented elsewhere for assessment, yet. The material used from other sources in this project and thesis have been properly acknowledged / referred. Report has been gone through plagiarism assessment.

Results of this assessment are attached.

Thermal Characterization and Management of Commercially Available Photovoltaic Cells

ORIGINALITY REPORT

9%

SIMILARITY INDEX

4%

INTERNET SOURCES

4%

PUBLICATIONS

3%

STUDENT PAPERS

PRIMARY SOURCES

1

Submitted to The Hong Kong Polytechnic University

Student Paper

2%

2

Submitted to Higher Education Commission Pakistan

Student Paper

1%

3

Bahaidarah, Haitham M.S.. "Experimental performance evaluation and modeling of jet impingement cooling for thermal management of photovoltaics", Solar Energy, 2016.

Publication

1%

4

Sajan Preet, Brij Bhushan, Tarun Mahajan. "Experimental investigation of water based photovoltaic/thermal (PV/T) system with and without phase change material (PCM)", Solar Energy, 2017

Publication

1%

5 www.dtic.mil 1%
Internet Source

6 www.incosol2012.ressol-medbuild.eu 1%
Internet Source

7 "Abstracts", Fuel and Energy Abstracts, 2016 1%
Publication

8 www.duo.uio.no 1%
Internet Source

9 Sourav Khanna, K.S. Reddy, Tapas K. Mallick. 1%
"Optimization of solar photovoltaic system
integrated with phase change material", Solar
Energy, 2018

Exclude quotes On
Exclude bibliography On

Exclude matches < 5 words

TABLE OF CONTENTS

ABSTRACT.....	3
ACKNOWLEDGMENTS.....	4
ORIGINALITY REPORT	5
LIST OF TABLES.....	iii
LIST OF FIGURES.....	iv
ABBREVIATIONS.....	v
NOMENCLATURE	v
CHAPTER 1: INTRODUCTION	1
CHAPTER 2: LITERATURE REVIEW	2
CHAPTER 3: METHODOLOGY	5
3.1 Light Source.....	5
3.2 Light Focusing Mechanism.....	5
3.3 Performance Parameters of PVs	7
3.4 Data Acquisition System.....	8
Thermal Characterization.....	11

3.5.1 PCM.....	13
Cost Analysis:	17
CHAPTER 4: RESULTS and DISCUSSIONS.....	18
4.1 Irradiance Distribution	18
4.4 Thermal Management	21
CHAPTER 5: CONCLUSION AND RECOMMENDATION.....	24
REFERENCES	25
APPENDIX I: Irradiance data for parabolic reflector.....	28

LIST OF TABLES

Table 1: Review of Solar Simulators	3
Table 2: Least count and uncertainty in instruments used	9
Table 3: Potential Materials to be used as PCM's	14
Table 4: Comparison of effect of different PCMs on temperature of PV cell	15

LIST OF FIGURES

Figure 1: Irradiance distribution for ellipsoidal reflector	6
Figure 2: Parabolic reflector and its light intensity distribution using APEX	7
Figure 3: Temperature measurement with AMG 88XX Sensor	11
Figure 4: Steady state thermal numerical simulation of a Si-PV cell	13
Figure 5: Numerical simulation for Si-Pv cell with Paraffin (C ₁₃ -C ₂₄)	16
Figure 6: Irradiance distribution of parabolic reflector.....	19
Figure 7: Thermal characterization at 1000 W/m ² & 1200 W/m ²	19
Figure 8: Efficiencies of Solar Cells at 1000 W/m ² & 1200 W/m ²	282
Figure 9: Output Power Density at 1000 W/m ² & 1200 W/m ²	28
Figure 10: Irradiance data of parabolic reflector at 43 cm from light source	28
Figure 11: Irradiance data of parabolic reflector at 45 cm from light source.....	28

ABBREVIATIONS

CBA	Computerized battery analyzer
FF	Fill factor
IR	Infrared
NI	National Instruments
PCM	Phase change material
PV	Photovoltaic

NOMENCLATURE

A	Area (m^2)
h	Heat transfer coefficient ($W/(m^2K)$)
I_{sc}	Short circuit current (A)
k	Thermal conductivity ($W/(m.K)$)
m_w	Mass of water (kg)
P	Power (W)
P_{max}	Maximum power (W)
Q_{cell}	Heat absorbed by cell (J)
\dot{Q}_{cell}	Rate of heat absorption by cell (W)
\dot{Q}_{conv}	Rate of heat convection (W)
\dot{Q}_{diss}	Rate of heat dissipation by PCM (W)
Q_{gen}	Heat generated due to light (J)
Q_{res}	Residual heat (J)
\dot{Q}_w	Rate of heat absorption by water (W)
T_{atm}	Atmospheric temperature ($^{\circ}C$)
T_{cell}	Cell temperature ($^{\circ}C$)
V_{oc}	Open circuit voltage (V)
η	Efficiency (%)

CHAPTER 1: INTRODUCTION

Photovoltaic cells are being used as an alternative power source in both power plants and in microgeneration of electricity. But it has been reported that during operation their temperature rises above the optimal temperature which results in gradual decrease in the output power and their conversion efficiencies. This creates need for comparison of different type of photovoltaic cells according to their response to variations in temperature. Also the need for different cooling methodologies to improve their efficiencies also arises.

The performance of photovoltaic modules shows a strong dependency on their temperature and this project aims to characterize different types of commercially available PV cells according to thermal behavior of their various performance parameters. A comparative study of application of different thermal management methodologies on performance of PV cells is also performed.

The objectives of this project include the testing of the simulator available in SMME for uniformity in irradiance distribution using pyranometry. If the solar simulator does not provide standard testing conditions for PV cells it will be modified and benchmarked for standardized study. The instrumentation of solar simulator for irradiance, temperature, current and voltage measurement will be done. The last objective of the project is to perform a comparative study of effect of different techniques to limit the increase in temperature of PV cells and thereby improving their efficiencies.

CHAPTER 2: LITERATURE REVIEW

Increase in global requirement for energy and the gradual decrease in the usage of hydrocarbons based fuels due to environmental pollution, have led to a rapid progression in installations of solar photovoltaics (PV) systems worldwide to as an alternative power source[1]. In 2015, less than 2% of global electricity was produced by PV with share of more than 7% from Italy, Germany and Greece[2], indicating that solar PV is still an emerging source of electrical power in global arena. Major drawbacks of solar PV include the inherent lower device level efficiency (typically $< 25\%$) at 25°C [3, 4] as well as degradation of power output and performance with rise in temperature of PV panels [5, 6] in outdoor operating conditions.

Commercially available mono-crystalline silicon photovoltaic cells have a reported efficiency of about 13-25% at an average surface temperature of 25°C [7]. The remaining power is utilized in heating the cell. The power output of PV and their conversion efficiency decrease with increasing temperature. Akhassi et al. studied effect of environmental factors including ambient temperature, solar irradiance and wind speed on the temperature of the solar cells and developed new models to determine temperature of PV module under different environmental conditions [8].

Solar simulators provide convenient way to study PV cells, solar thermal collectors, and thermochemical processes [10, 11] as they can offer light with similar spectral composition to sunlight [10] and intensities in range of less than 1 sun ($1000\text{W}/\text{m}^2$) [12] to more than 2000 suns [11], without interruptions caused by environmental factors as in case of testing under natural sunlight [13, 14]. Solar simulators are also being used for development and testing of various thermal management methodologies to improve performance of solar cells.

Table 1: Review of Solar Simulators

Light Source	Power Rating/ Lamp (kW)	Focusing Mechanism	Results	References
Xenon Arc	7	Fresnel Lens	Peak flux of 6.73 MW/m ² on a 20 cm diameter target	Wang, et al. [15]
	5	Ellipsoidal Mirror And Fresnel Lens	Average Flux of 24.3 kW/m ²	Okuhara, et al. [16]
	15	Array of Ellipsoidal Reflectors with common focus	Average Flux of 6800 kW/m ² on 60 mm diameter area	Petrasch, et al. [17]
LED	Nil	Nil	Average Flux of 590 W/m ² on a 38 x 38 cm ² area	Bliss, et al. [18]
	Nil	Nil	10 W/m ² with 3% uniformity on 21 x 21 cm ² area	Kohraku and Kurokawa [19]
Metal Halide Lamp	6	Ellipsoidal Reflector	Peak Flux of 927 kW/m ² on a 17.5 cm area	Ekman, et al. [20]
	1.5	Conical Concentrator	Peak flux of 60 kW/m ² Average flux of 45 kW/m ²	Codd, et al. [21]
	1.5, 2.5, 4	Ellipsoidal Reflector	Adjustable Flux of 429-858 kW/m ²	Roba and Siegel [22]

The temperature of PV cells has been reported to go as high as 80⁰C during operating conditions and this increase in temperature has been shown to have an insignificant dependence on surrounding temperature, but a strong dependence upon solar irradiance, wind speed and material properties of PV module [23]. Klugmann et. al has shown that for mono crystalline cells, the output power decreases and conversion efficiency of device drops by 0.65% and 0.08% for every 1⁰C increase in the temperature of the solar cell [7].

Several thermal management methodologies were employed by researchers to limit the increase in temperature and improve device performance. Cuce et. al used aluminum fins to increase rate of heat transfer to the environment and an increase in output power of about

20% was achieved [24]. Thermodynamic performance of silicon PV cells was enhanced with help of air cooling [25]. Back surface water cooling was used by Bahaidarah et. al and an increase in efficiency of 9% was achieved by decreasing temperature by 20% [26]. Phase change materials have also been used to improve cell efficiency where PCM absorbs heat from cell as heat of fusion and increase in temperature is avoided. Mousavi et al. achieved a temperature drop of 15°C by using polyethylene glycol as a PCM [27]. RT27 PCM with internal aluminum fins for enhanced heat transfer from PV module to PCM was used by Huang et. al [28]. A decrease in the temperature of 20°C was achieved for a building integrated PV module resulting in an increase of 10% in electrical efficiency of the module.

CHAPTER 3: METHODOLOGY

This section the performance parameters of PV cells along with the testing and improvement of solar simulator, and design of data acquisition systems and thermal management techniques. Solar simulator must provide some necessary and standard testing conditions.

These conditions include:

1. An average irradiance of 800-1000 W/m² on testing plane with non-uniformity of 2% in class A simulators, 5% in class B simulators and 10% in class C simulators.
2. Spectral distribution of simulator should match the spectrum of sun.

The components of solar simulator include a light source with spectral distribution similar to that of sun, a light focusing mechanism which provides a uniform distribution of irradiance on the PV cell.

3.1 Light Source

The irradiance of sun on earth varies greatly depending upon positioning with respect to sun and weather conditions. This makes it difficult to test PV cells under sunlight. For laboratory testing a uniform light source with a spectrum that matches the spectral distribution of sun is required. Dong et. al have shown that spectrum of metal halide lamp matches the spectrum of sun most closely [29]. Metal halide lamp was used selected as a light source. The solar simulator available in SMME also used a metal halide lamp. After market survey it was found that the lamps available in market were tube shaped and cannot be used with the truncated ellipsoidal simulator available.

3.2 Light Focusing Mechanism

The simulator already available in SMME used a truncated ellipsoidal reflector as a light focusing mechanism. It worked on the principle that when a point source of light is

placed at one focus of ellipsoid, rays of light after reflecting from the surface of reflector are focused on the secondary focus of truncated ellipsoidal reflector. When a spherical light source is used an axial symmetric distribution is obtained. The metal halide lamp used in the simulator was tube shaped and hence the irradiance distribution was highly non-uniform.

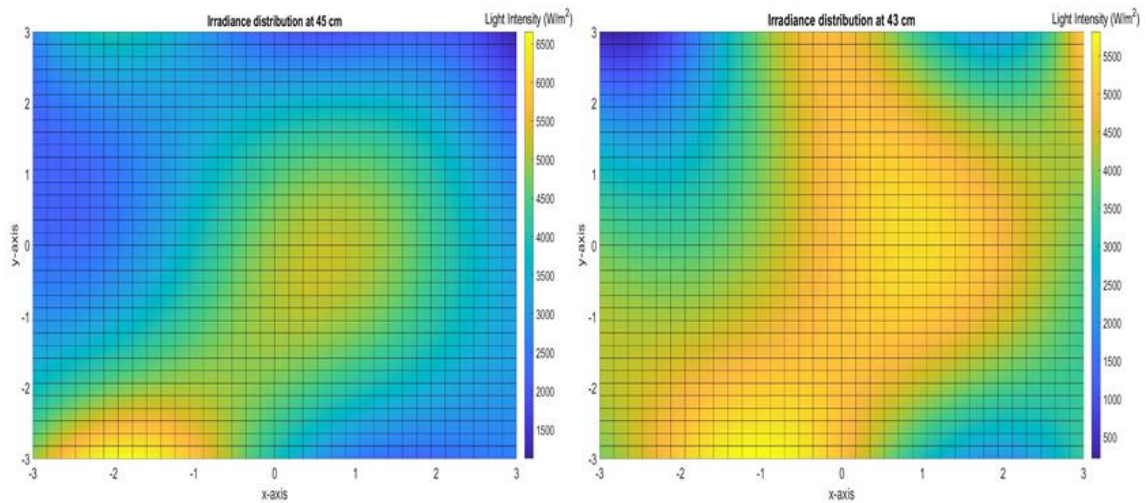


Figure 1: Irradiance distribution for ellipsoidal reflector

After testing of simulator with help of a CM4 pyranometer by Kipp & Zonen, it was found that the intensity distribution did not lie in any of the prescribed classes of solar simulators. Figure 1 shows the irradiance measured in an area of $6 \times 6 \text{ cm}^2$ at two planes one at 45 cm distance from light source and other at 43 cm. Due to large non-uniformities in irradiance distribution of truncated ellipsoidal reflector it is not suitable for testing of PV cells. Hence a new light focusing mechanism has to be designed.

A parabolic dish reflector was designed to achieve uniformity in irradiance distribution. This type of concentrator is based on the geometric properties of a parabola. The rays of light emitting at the focus of a parabola after being reflected from its surface, become parallel. The parabolic reflector designed using APEX-Solidworks and its predicted

irradiance distribution is shown in figure 2. It can be seen that the intensity is less uniform directly under the metal halide lamp, but as we move away from arc it becomes more uniform.

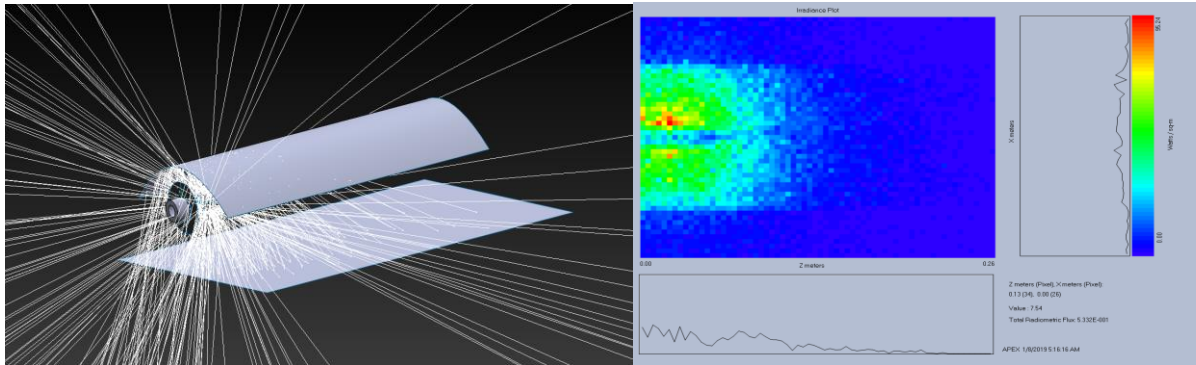


Figure 2: Parabolic reflector and its light intensity distribution using APEX

3.3 Performance Parameters of PVs

3.3.1 Short Circuit Current

Without any incident light a solar cell shows the same characteristics as that of a diode. Short circuit current is the maximum current which can flow through the solar cell when the potential difference is zero, and is produced due to generation and collection of charge carriers in PV cell. It depends upon, optical properties of solar cell, light spectrum and the area of solar cell and that is why instead of current, current density is used.

3.3.2 Open Circuit Voltage

It is the maximum value of potential difference available for a photovoltaic cell and occurs when the circuit is open or the current flow through circuit is zero. It depends upon saturation current of PV and also on the light generated current.

3.3.3 Maximum Power

It is the maximum power that can be extracted from the cell under particular conditions (temperature and light intensity).

$$P_m = (FF)I_{sc}V_{oc}$$

3.3.5 Efficiency

It is the ratio of maximum electrical power from the cell to the total irradiance power on the cell.

$$\eta = \frac{P_{max}}{Irradiance\ Power}$$

Where

$$Irradiance\ Power = Average\ irradiance * Area\ of\ cell$$

3.4 Data Acquisition System

The data acquisition system consists of a temperature measurement system, a current-voltage and power-voltage curve tracing mechanism and an irradiance measurement system.

3.4.1 Irradiance Measurement

For measurement of the light intensity the CM4 pyranometer by Kipp & Zonen is used. This pyranometer provides a high operational temperature range of -40 to +150 °C, and a response time of less than 8 seconds. The irradiance from lamp was measured in an area of 6*6 cm² at 36 points.

Table 2: Least count and uncertainty in instruments used

Instrument	Least Count	Uncertainty
Pyranometer	66.61 W/m ²	±2.58 %
Voltmeter	0.01 mV	±0.5%

3.4.2 I-V and P-V curve tracer

Current-voltage curve for PV cells is used to obtain their different performance parameters such as maximum power point, fill factor and conversion efficiency of the cell. It can be obtained by sweeping load across the PV cell from open circuit condition (infinite resistance) to short circuit condition (zero resistance). This was done by manual variation in resistance across the cell with help of a potentiometer and measurement of current and voltage using in parallel and ammeter in series to the solar cell, respectively.

3.4.3 Temperature Measurement

The temperature of the cell has to be measured at both the irradiated and dark surfaces. At the dark surface thermocouples can be used. But at irradiated surfaces, the temperature measurements cannot be taken using thermocouples as they will block the light. Hence an AMG88XX sensor along with raspberry pi is used for temperature measurements. The sensor needs to be calibrated and its calibration was performed using a Fluke tis45 infrared temperature gun. A hot plate was used, and its temperature was varied and measured with both Fluke temperature gun and AMG88XX sensor. The AMG88XX sensor measures

temperature in a 64 pixels square grid. Its height has to be adjusted such as to achieve a high resolution on the cell surface.

The temperature measurement system consists of thermocouples at the dark surface of cell and an infrared temperature sensor at the irradiated surface of the cell. Figure 6 shows the comparison of temperature measurements using AMG88XX sensor. It can be seen that the temperature measured using the sensor is sufficiently close to the actual temperature of the heat plate, and the temperature measured using Fluke IR temperature gun. The resolution of the sensor can be varied by changing the distance between the cell and sensor and also by coupling two sensors thus increasing the grid for 64 pixels to 128 pixels.

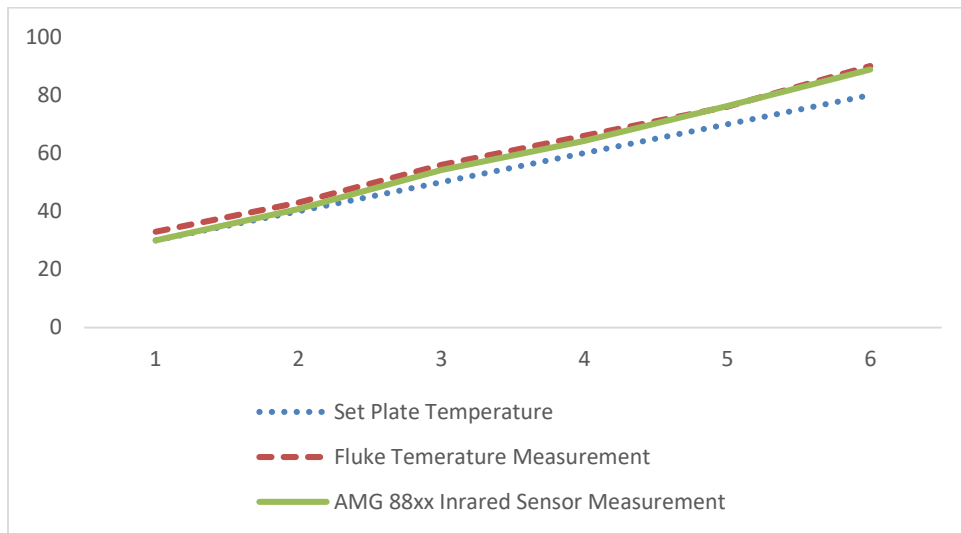


Figure 3: Temperature measurement with AMG 88XX Sensor

Thermal Characterization

Different types of commercially available PV cells were characterized with respect to their performance and the impact of temperature on it. Mono-crystalline, two types of polycrystalline and thin film cells were selected. The cells were selected on the basis of maximum power output per unit area available in the particular class. Characterization was performed at two intensities, i.e 1000 W/m^2 and 1200 W/m^2 , to study the impact of increase in light intensity on solar cell. The solar cell was placed in the simulator and when steady state was achieved with respect to both light intensity and temperature the current, voltage and power output of the cell were measured. The temperature of the cell was measured on the irradiated surface with help of an infrared temperature sensor and on the dissipative side of cell with two thermocouples.

3.5 Thermal Management

Thermal management of photovoltaic cells is required due to the fact that their efficiency and power output decrease with increase in temperature. Different types of thermal management methodologies are employed by researchers to improve cell performance. These methods include usage of fins, phase change materials, water and air cooling, heat pipes, micro-channel heat sinks and cooling using Nano-fluids. In this study a comparison of four methods of controlling temperature of PV cells are used including fins, water jacket, thermo-electric generator and phase change materials.

The steady state thermal analysis was performed for a Silicon based solar cell under a solar irradiance of $1000\text{W}/\text{m}^2$ and ambient temperature of 25°C . The modes of heat transfer considered were radiative and natural convective heat transfer from the irradiated and dark surfaces of PV cell. It was found using analytical solution of heat transfer problem that the temperature of PV cell goes as high as 91.26°C and the numerical simulation was also performed using steady state analysis in ANSYS as shown in figure 7. The results show that the temperature of cell reaches 93.78°C at steady state.

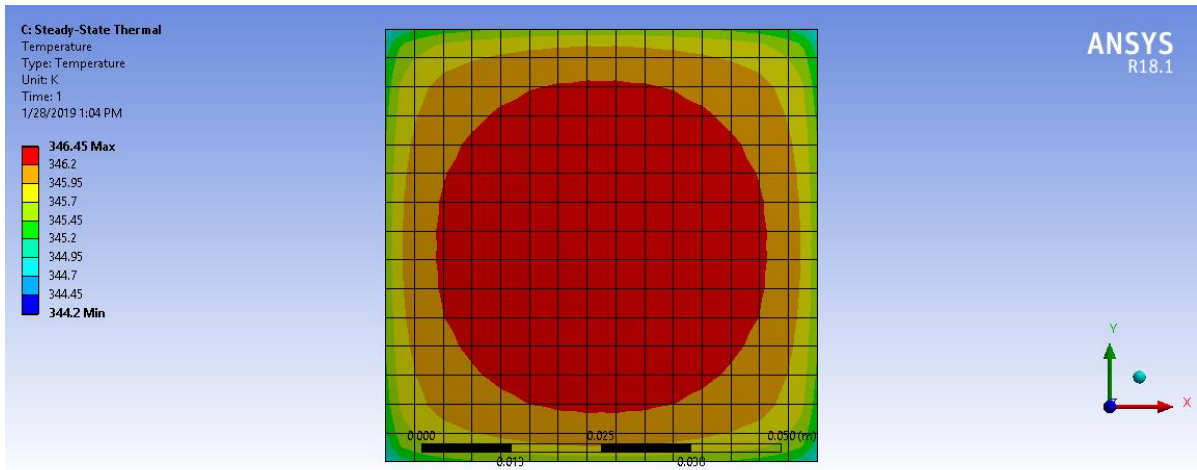


Figure 4: Steady state thermal numerical simulation of a Si-PV cell

3.5.1 PCM

One of the techniques used for passive thermal management of photovoltaic cells is the use of phase change materials for maintaining the temperature of the solar panel to a desirable value. A phase change material is characterized by high latent heat of fusion i.e. it absorbs a large amount of heat at a constant temperature during phase change process.

Table 3: Potential Materials to be used as PCM's [30-33]

Material	Type	Melting Temperature (°C)	Heat of Fusion (kJ/kg)	Thermal Conductivity(W/mK)
Paraffin C ₁₆ -C ₁₈	Organic	20-22	152	-
Paraffin C ₁₃ -C ₂₄	Organic	22-24	189	0.21
Paraffin C ₁₈	Organic	28	244	0.15
CaCl ₂ .6H ₂ O(Hydrated Salt)	Inorganic	29.7	171	-
RT-25		25	147	1.02

For application on solar panel, the most desirable phase change temperature is around 22-25°C and thermal conductivity should be as high as possible since PCM is in contact at the back surface of the solar panel and it must be capable of absorbing heat from the front surface and thermal contact resistance should be as much minimized as possible. Paraffins are usually used with PV cells due to their melting temperature closer to the optimum working temperature of PV cells. Another potential category of PCM's are hydrated salts because they have very low prices and they are light weight making it easy to handle them. Rubitherms too prove themselves to be a valuable class of materials for phase change processes as they can be designed to have the desired melting point while having required latent heat and thermal conductivity properties. Rubitherm PCM's are innovative phase change materials based on paraffin and waxes for the effective storage of sensible and latent heat. Some of the potential materials in this respect are as given in table 3.

The phase change materials absorb a large amount of heat equal to their heat of fusion to change phase from solid to liquid while maintaining a constant temperature. Hence they help in limiting the increase in temperature of PV cell.

Q_{gen} is the component of total light energy available to solar cell which is converted into heat.

$$Q_{gen} = \text{Irradiance} * \text{surface area of cell} * \text{efficiency of cell}$$

Q_{res} is the residual heat which remains in solar cell after some of its heat energy has been removed by PCM.

$$Q_{res} = h * A * \Delta t * (T_{cell} - T_{atm})$$

Table 4: Comparison of effect of different PCMs on temperature of PV cell

	Steady state Temperature	Temperature With PCM (°C)		
PCM	Without PCM	after 1 hour	after 2 hours	after 3 hours
Paraffin C ₁₃ -C ₂₄	91.26	25	45.7438	61.4938
Paraffin C ₁₈		25	31.9938	52.3271
CaCl ₂ .6H ₂ O (Hydrated Salt)		25	50.2438	64.4938
RT-25		25	41.6604	58.7716

A comparison of different PCMs for cooling of PV cell is shown in table 4. It can be seen that without using a PCM the temperature of the cell goes as high as 93°C. Also the temperature remains at the ambient temperature for first hour, but it starts increasing after that. The result show that the Paraffin (C₁₈) causes the maximum drop in temperature and will improve the efficiency of PV cell most significantly. It can be seen at start this rate

is low as most of the heat absorbed by cell is being utilized by Paraffin to change its phase.

Once the phase change is complete the rate of increase in temperature of cell increases.

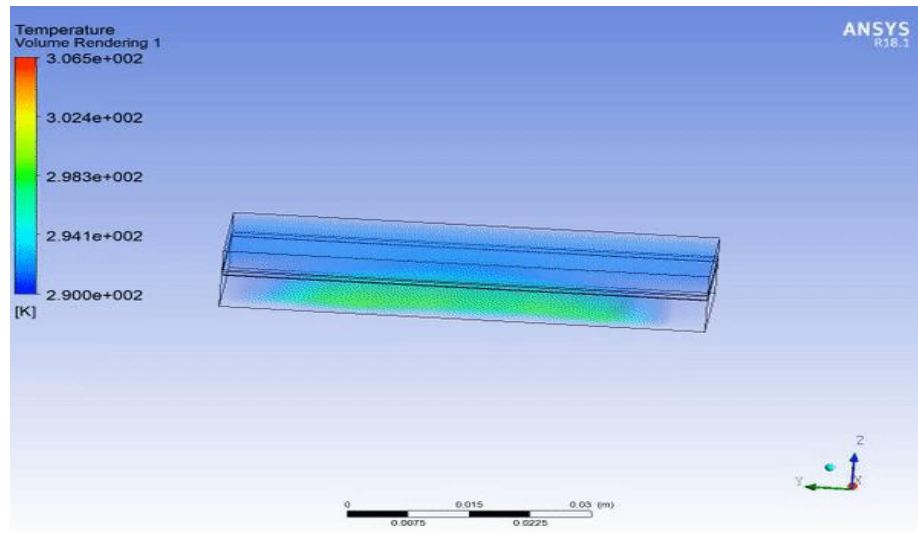


Figure 5: Numerical simulation for Si-PV cell with Paraffin (C13-C24)

COST ANALYSIS:

The Phase change material used for evaluation was Modified Paraffin Wax and calculations for paraffin wax are as follows:

PCM Type	Density	Price \$ per kg
Modified Paraffin Wax	900	1.89

The results of the calculations are as follows and the detail is provided in Appendix.

Volume Req. (m3)	0.906553846
mass of pcm req. (kg)	815.8984615
Price of Req. PCM	1542.048092
Price of PCM per watt	0.514016031
Price per watt (without including the price of pcm)	0.449655461
Total price per watt	0.963671492

To conclude Paraffin Wax is only financially feasible if area is a constraint. Otherwise, added cost of Paraffin wax is greater than the added benefit of greater efficiency. Likewise, fins could only be beneficial if area is a constraint. Otherwise added cost with outweigh the increase in efficiency.

CHAPTER 4: RESULTS AND DISCUSSIONS

This chapter presents and discusses results for irradiance distribution of improved solar simulator, testing of I-V and P-V curve tracing systems. The comparison of temperature measurement from Fluke temperature gun and infrared temperature sensor is also provided. Effect of applying different cooling techniques on the temperature of PV cell is also determined.

4.1 Irradiance Distribution

The irradiance distribution of the parabolic reflector based simulator, in an area of $6*6 \text{ cm}^2$, at two levels is shown in figure 7. This was plotted using a 14 degree interpolation polynomial. The results show that the uniformity in irradiance has highly enhanced. At a distance of 45 cm from the light source the average irradiance is 1180.70 W/m^2 with a standard deviation of 30.51 which is a large improvement in the uniformity over the ellipsoidal reflector. This can be attributed to the fact that the rays of light from the tube shaped light source placed along the focal line of parabolic reflector become parallel after reflecting from the reflector. The non-uniformity of the solar simulator is about 7% and hence it falls under the class C of the solar simulators as mentioned above. For irradiance data see appendix I.

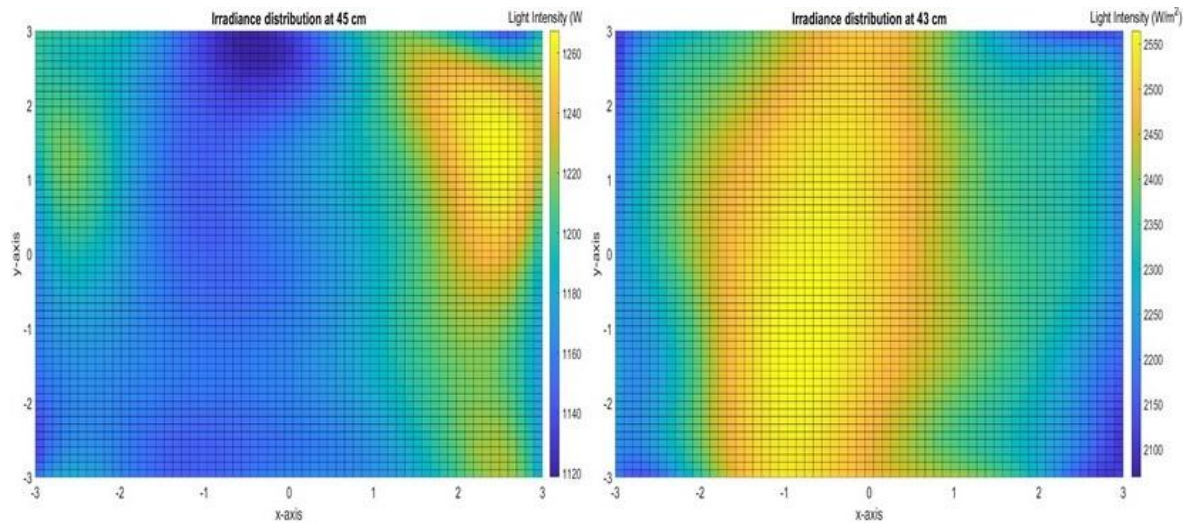


Figure 6: Irradiance distribution of parabolic reflector

Thermal Characterization

Thermal characterization of performance of different types of commercially available photovoltaic cells was performed at two different intensity levels. Figure 8 a and b show the power density of different types of cells at 1000 and 1200 W/m² respectively. It can be seen that the maximum output power density was obtained for poly-crystalline cells of type B. The thin film cells as shown have the minimum output power density among the four cells tested.

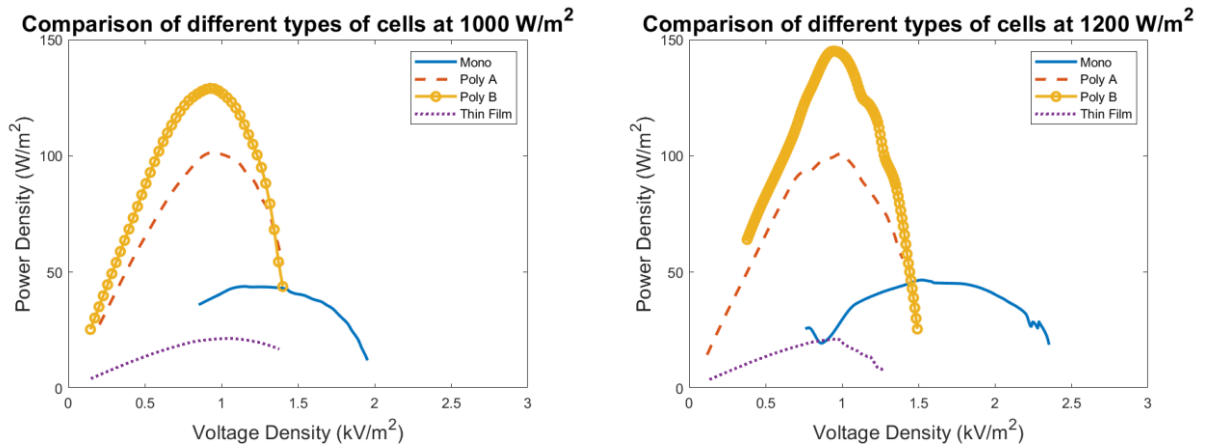


Figure 7: Thermal characterization at a) 1000 W/m² b) 1200 W/m²

Summary of the data for characterization of PV cells is provided in table XYZ. T_{amb} represents the ambient temperature during test. $T_{rad-cell}$ is the average temperature at the irradiated surface of the solar cell. It is measured at sixteen random points on the cell surface with the help of AMG8833 infrared temperature measurement sensor. The $T_{diss-cell}$ represents the average temperature at the dissipative surface of the cell measured using two k-type thermocouples. Cells are characterized with respect to the power density to eliminate the effect of variation in total available PV area of cell due to their different sizes. It may be noted that the maximum power output of the cell increases with increase in temperature but the conversion efficiency of cell decreases. Also, it may be noted that the poly-crystalline cells give the maximum efficiency among the group even at relatively higher temperatures.

Class	1000 W/m ²				1200 W/m ²			
	Mono-crystalline	Poly-crystalline A	Poly-crystalline B	Thin film	Mono-crystalline	Poly-crystalline A	Poly-crystalline B	Thin film
Area cm ²	4.5	3.42	3.42	27.54	4.5	3.42	3.42	27.54
T _{amb} C	39.95	40.43	39.5	39.08	41.72	42.08	42.19	40
T _{rad-cell} C	75.9	90.84	86.89	82.87	82.77	83.77	82.80	83
T _{diss-cell} C	69.94	66.91	73.47	59.36	62.37	57.38	65.87	61.67
Max power density kW/m ²	43.87	101.57	129.07	23.18	53.61	101.02	145.09	24.86
Efficiency %	4.43	10.2	12.88	1.922	4.04	7.47	12.10	1.81

4.4 Thermal Management

Thermal management of PV cells was performed using two different passive cooling techniques i.e., fins and phase change material. The results show that a larger drop in temperature of cell was observed with application of phase change materials as compared with fins that results in relatively larger enhancement in power output and efficiency of cells.

Figure 9 a and b represent the effect of application of fins and Paraffin Wax PCM on different types of cells. It can be seen than with application of thermal management systems the light to electrical conversion efficiency of solar cells increases. The poly crystalline cells of type 1 show maximum increase in efficiency due to decrease in temperature. An increase in conversion efficiency from 10.20 to 21.82 is observed for these cells due to decrease in temperature with application of phase change material.

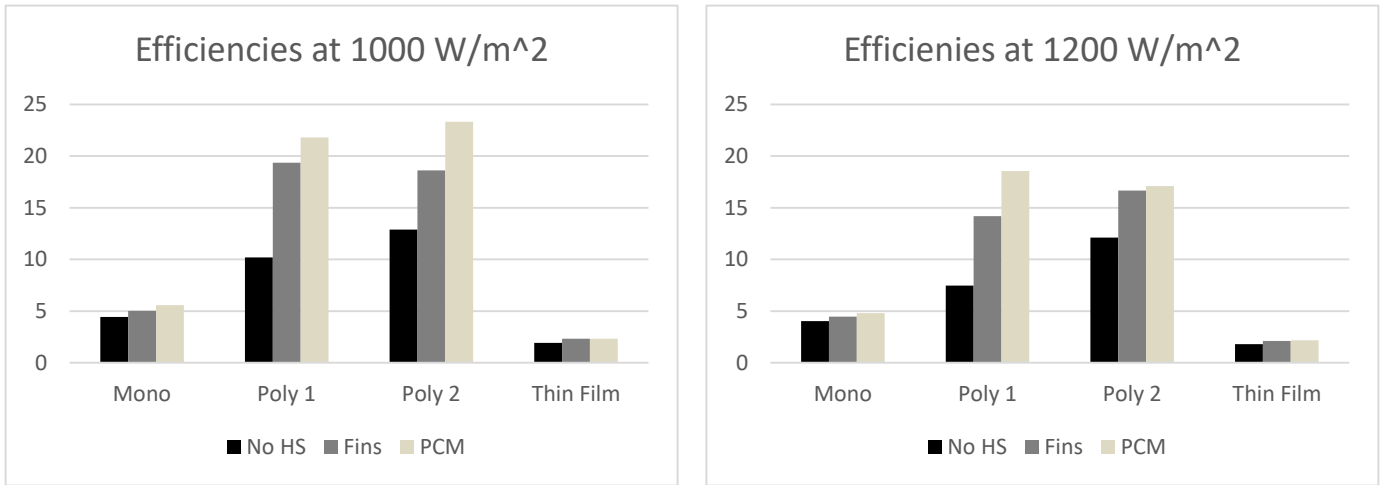


Figure 8: Efficiencies of Solar Cells at a) 1000 W/m² b) 1200 W/m²

Figure 10 (a) and (b) represent the effect of application of different types of passive cooling techniques on the power output of solar cells. It can be seen that the polycrystalline cells of type 2 show maximum output power density without application of any cooling methodology. However, the maximum relative increase in output power density exists for the polycrystalline cells of type 1 when phase change material is employed as a cooling method. It can also be seen that with increase in light intensity the maximum output power of cell increases but its solar power to electrical power conversion efficiency decreases. Also that the effect of thermal management methodologies on the electrical performance parameters of thin films PV cells is negligible.

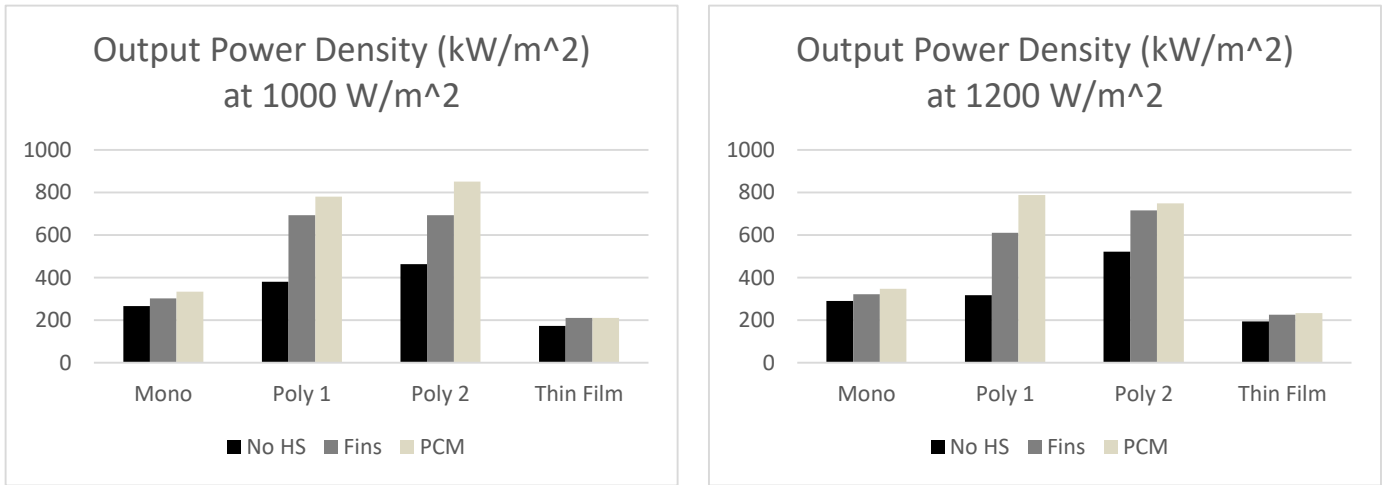


Figure 9: Output Power Density at a) 1000 W/m² b) 1200 W/m²

The polycrystalline cells of type 2 are recommended to be used when no heat sinks or cooling methods are to be applied. On the other hand, when heat sinks are used the polycrystalline cells of type 1 must be used to gain maximum output power per unit area of cell.

CHAPTER 5: CONCLUSION AND RECOMMENDATION

The solar simulator design is improved for standardized testing of photovoltaic cell. It consists of a 1000 W tube shaped metal halide lamp coupled with a parabolic reflector for uniform distribution of irradiance. It can provide a wide irradiance range of 800 to 2500 W/m² with less than 7% uncertainty and lies in the class C of solar simulators, as defined by ASTM. The data acquisition system consisting of irradiance measurement, current and voltage measurements and temperature measurements has been made. Different types of commercially available PV cells were characterized on basis of their performance with change in temperature. It was found that the polycrystalline cells give maximum power output per unit area among all the cell types considered. Thermal management of cells was performed using both fins and phase change materials and at 1000 W/m² an increase in efficiency of 1.13% occurred for monocrystalline cells, 11.61% for polycrystalline type 1, 10.43% for polycrystalline 2, and 0.4152% for thin film cells. At light intensity of 1200 W/m² the efficiency of monocrystalline cells increases by 0.77%, of polycrystalline cells of type 1 by 11.07%, of polycrystalline type 2 by 5% and of thin film cells by 0.36%. Polycrystalline cells show the maximum power output per unit area and hence are recommended to be used for commercial purposes. Also in case of limited space thermal management methods can be utilized to further improve the power output per unit area.

REFERENCES

- [1] B. Kumar Sahu, "A study on global solar PV energy developments and policies with special focus on the top ten solar PV power producing countries," *Renewable and Sustainable Energy Reviews*, vol. 43, pp. 621-634, 2015.
- [2] S. K. Kar, A. Sharma, and B. Roy, "Solar energy market developments in India," *Renewable and Sustainable Energy Reviews*, vol. 62, pp. 121-133, 2016/09/01/ 2016.
- [3] V. V. Tyagi, N. A. A. Rahim, N. A. Rahim, and J. A. L. Selvaraj, "Progress in solar PV technology: Research and achievement," *Renewable and Sustainable Energy Reviews*, vol. 20, pp. 443-461, 2013.
- [4] T. M. Razykov, C. S. Ferekides, D. Morel, E. Stefanakos, H. S. Ullal, and H. M. Upadhyaya, "Solar photovoltaic electricity: Current status and future prospects," *Solar Energy*, vol. 85, no. 8, pp. 1580-1608, 2011.
- [5] E. Radziemska, "The effect of temperature on the power drop in crystalline silicon solar cells," *Renewable Energy*, vol. 28, no. 1, pp. 1-12, 2003.
- [6] A. Q. Malik and S. J. B. H. Damit, "Outdoor testing of single crystal silicon solar cells," *Renewable Energy*, vol. 28, no. 9, pp. 1433-1445, 2003.
- [7] E. Klugmann-Radziemska, *The effect of temperature on the power drop in crystalline solar cells*. 2003, pp. 1-12.
- [8] M. Akhsassi *et al.*, "Experimental investigation and modeling of the thermal behavior of a solar PV module," *Solar Energy Materials and Solar Cells*, vol. 180, pp. 271-279, 2018/06/15/ 2018.
- [9] W. Yuan *et al.*, "Comparison study of the performance of two kinds of photovoltaic/thermal(PV/T) systems and a PV module at high ambient temperature," *Energy*, vol. 148, pp. 1153-1161, 2018/04/01/ 2018.
- [10] W. Wang and B. Laumert, "Simulate a 'sun' for solar research: a literature review of solar simulator technology," ed: KTH Royal Institute of Technology, 2014.
- [11] A. Gallo, A. Marzo, E. Fuentealba, and E. Alonso, "High flux solar simulators for concentrated solar thermal research: A review," *Renewable and Sustainable Energy Reviews*, vol. 77, pp. 1385-1402, 2017/09/01/ 2017.
- [12] A. Namin, C. Jivacate, D. Chenvidhya, K. Kirtikara, and J. Thongpron, "Determination of solar cell electrical parameters and resistances using color and white LED-based solar simulators with high amplitude pulse input voltages," *Renewable Energy*, vol. 54, pp. 131-137, 2013.
- [13] A. Guechi and M. Chegaar, "Effects of diffuse spectral illumination on microcrystalline solar cells," *J. Electron Devices*, vol. 5, pp. 116-121, 2007.

- [14] V. Esen, Ş. Sağlam, and B. Oral, "Light sources of solar simulators for photovoltaic devices: A review," *Renewable and Sustainable Energy Reviews*, vol. 77, pp. 1240-1250, 2017/09/01/ 2017.
- [15] W. Wang, L. Aichmayer, B. Laumert, and T. Fransson, "Design and Validation of a Low-cost High-flux Solar Simulator using Fresnel Lens Concentrators," *Energy Procedia*, vol. 49, pp. 2221-2230, 2014/01/01/ 2014.
- [16] Y. Okuhara, T. Kuroyama, T. Tsutsui, K. Noritake, and T. Aoshima, "A Solar Simulator for the Measurement of Heat Collection Efficiency of Parabolic Trough Receivers," *Energy Procedia*, vol. 69, pp. 1911-1920, 2015/05/01 2015.
- [17] J. r. Petrasch *et al.*, "A Novel 50 kW 11,000 suns High-Flux Solar Simulator Based on an Array of Xenon Arc Lamps," *Journal of Solar Energy Engineering*, vol. 129, no. 4, p. 405, 2007.
- [18] M. Bliss, T. R. Betts, and R. Gottschalg, "An LED-based photovoltaic measurement system with variable spectrum and flash speed," *Solar Energy Materials and Solar Cells*, vol. 93, no. 6, pp. 825-830, 2009/06/01/ 2009.
- [19] S. Kohraku and K. Kurokawa, "New methods for solar cells measurement by LED solar simulator," in *3rd World Conference on Photovoltaic Energy Conversion, 2003. Proceedings of*, 2003, vol. 2, pp. 1977-1980 Vol.2.
- [20] B. M. Ekman, G. Brooks, and M. Akbar Rhamdhani, "Development of high flux solar simulators for solar thermal research," *Solar Energy Materials and Solar Cells*, vol. 141, pp. 436-446, 2015.
- [21] D. Codd, A. Carlson, J. Rees, and A. Slocum, *A low cost high flux solar simulator*. 2010, pp. 2202-2212.
- [22] J. P. Roba and N. P. Siegel, "The design of metal halide-based high flux solar simulators: Optical model development and empirical validation," *Solar Energy*, vol. 157, pp. 818-826, 2017/11/15/ 2017.
- [23] S. Dubey, J. N. Sarvaiya, and B. Seshadri, "Temperature Dependent Photovoltaic (PV) Efficiency and Its Effect on PV Production in the World – A Review," *Energy Procedia*, vol. 33, pp. 311-321, 2013/01/01/ 2013.
- [24] E. Cuce, T. Bali, and S. A. Sekucoglu, "Effects of passive cooling on performance of silicon photovoltaic cells," *International Journal of Low-Carbon Technologies*, vol. 6, no. 4, pp. 299-308, 2011.
- [25] E. Cuce and P. M. Cuce, "Improving thermodynamic performance parameters of silicon photovoltaic cells via air cooling," *International Journal of Ambient Energy*, vol. 35, no. 4, pp. 193-199, 2014/10/02 2014.
- [26] H. Bahaidarah, A. Subhan, P. Gandhidasan, and S. Rehman, "Performance evaluation of a PV (photovoltaic) module by back surface water cooling for hot climatic conditions," *Energy*, vol. 59, pp. 445-453, 2013/09/15/ 2013.

- [27] S. R. Mousavi Baygi and S. M. Sadrameli, "Thermal management of photovoltaic solar cells using polyethylene glycol 1000 (PEG1000) as a phase change material," *Thermal Science and Engineering Progress*, vol. 5, pp. 405-411, 2018/03/01/ 2018.
- [28] M. J. Huang, P. C. Eames, B. Norton, and N. J. Hewitt, "Natural convection in an internally finned phase change material heat sink for the thermal management of photovoltaics," *Solar Energy Materials and Solar Cells*, vol. 95, no. 7, pp. 1598-1603, 2011/07/01/ 2011.
- [29] X. Dong, Z. Sun, G. J. Nathan, P. J. Ashman, and D. Gu, "Time-resolved spectra of solar simulators employing metal halide and xenon arc lamps," *Solar Energy*, vol. 115, pp. 613-620, 2015/05/01/ 2015.
- [30] P. H. Biwole, P. Eclache, and F. Kuznik, "Phase-change materials to improve solar panel's performance," *Energy and Buildings*, vol. 62, pp. 59-67, 2013/07/01/ 2013.
- [31] C. Mehling, *Heat and cold storage with PCM*, 1 ed. Heidelberg: Springer-Verlag Berlin 2008, p. 308.
- [32] V. V. Tyagi and D. Buddhi, "PCM thermal storage in buildings: A state of art," *Renewable and Sustainable Energy Reviews*, vol. 11, no. 6, pp. 1146-1166, 2007/08/01/ 2007.
- [33] B. Zalba, J. M. Marín, L. F. Cabeza, and H. Mehling, "Review on thermal energy storage with phase change: materials, heat transfer analysis and applications," *Applied Thermal Engineering*, vol. 23, no. 3, pp. 251-283, 2003/02/01/ 2003.

APPENDIX I: IRRADIANCE DATA FOR PARABOLIC

REFLECTOR

		X-axis						
		-3	-2	-1	0	1	2	3
Y-axis	-3	1155.116	1148.515	1161.716	1168.317	1188.119	1201.32	1207.921
	-2	1161.716	1161.716	1168.317	1174.917	1181.518	1181.518	1194.719
	-1	1148.515	1155.116	1155.116	1148.515	1148.515	1141.914	1135.314
	0	1161.716	1161.716	1161.716	1161.716	1168.317	1148.515	1141.914
	1	1168.317	1181.518	1188.119	1188.119	1194.719	1201.32	1207.921
	2	1207.921	1214.521	1221.122	1234.323	1247.525	1254.125	1247.525
	3	1161.716	1155.116	1161.716	1174.917	1201.32	1221.122	1227.723

Figure 10: Irradiance data of parabolic reflector at 45 cm from light source

		X-axis						
		-3	-2	-1	0	1	2	3
Y-axis	-3	2198.02	2244.224	2244.224	2231.023	2211.221	2165.017	2125.413
	-2	2363.036	2402.64	2409.241	2435.644	2429.043	2389.439	2310.231
	-1	2534.653	2554.455	2561.056	2547.855	2528.053	2488.449	2429.043
	0	2468.647	2488.449	2514.851	2521.452	2521.452	2508.251	2495.05
	1	2409.241	2382.838	2415.842	2409.241	2409.241	2389.439	2376.238
	2	2270.627	2290.429	2330.033	2343.234	2336.634	2336.634	2330.033
	3	2125.413	2118.812	2178.218	2184.818	2191.419	2184.818	2178.218

Figure 11: Irradiance data of parabolic reflector at 43 cm from light source

Table 5: Thermal management of different types of cells at 1000 W/m²

Cell Type		T amb	T rad	T dis-cell	T dis_HS	Pmax	Efficiency
Mono	No HS	39.95	75.90	69.94	-	266.19	4.43
	Fins	40.50	65.00	49.96	42.81	302.41	5.03
	PCM	40.10	63.50	52.50	44.00	333.66	5.57
Poly 1	No HS	40.43	90.85	66.92	-	380.33	10.20
	Fins	40.17	66.65	58.83	37.29	694.14	19.36
	PCM	40.50	63.90	52.83	62.45	781.12	21.81
Poly2	No HS	39.50	86.89	73.47	-	462.81	12.89
	Fins	40.10	63.50	55.00	41.29	694.00	18.63
	PCM	40.58	61.30	52.54	48.88	852.00	23.32
Thin Film	No HS	39.08	82.88	59.36	-	173.85	1.92
	Fins	39.42	60.00	54.88	48.71	210.10	2.33
	PCM	39.75	57.43	52.25	48.33	211.08	2.34

Table 6: Thermal management of different types of cells at 1200 W/m²

Cell Type		T amb	T rad	T dis-cell	T dis_HS	Pmax	Efficiency
Mono	No HS	41.72	82.77	62.38	-	291.17	4.04
	Fins	38.92	66.57	53.00	42.79	322.57	4.47
	PCM	38.90	66.57	51.00	42.00	347.90	4.82
Poly 1	No HS	42.08	83.77	57.39	0.00	318.00	7.48
	Fins	40.08	69.19	61.42	49.58	610.76	14.20
	PCM	40.42	62.45	54.92	0.00	789.26	18.55
Poly2	No HS	42.19	82.80	65.88	0.00	521.67	12.11
	Fins	40.08	66.31	63.38	48.54	717.00	16.68
	PCM	40.58	57.76	53.04	43.21	749.32	17.11
Thin Film	No HS	40.00	83.00	61.67	0.00	194.33	1.81
	Fins	40.92	64.45	55.67	43.67	226.40	2.11
	PCM	40.92	58.92	52.92	49.00	233.45	2.18